https://doi.org/10.1016/j.atmosres.2020.105398

Review of Dust Storm Detection Algorithms for Multispectral Satellite Sensors

Jing Li[1], Man Sing Wong[1]*, Kwon Ho Lee[2], Janet Nichol[3], PW Chan[4]

[1] Department of Land Surveying and Geo-Informatics, The Hong Kong Polytechnic University, Hong Kong, China (email: jenne.li@connect.polyu.hk; Ls.charles@polyu.edu.hk)
[2] Department of Atmospheric & Environmental Sciences, Gangneung-Wonju National University, Korea (email: kwonho.lee@gmail.com)
[3] School of Global Studies, University of Sussex, U.K. (email: jen27@sussex.ac.uk)
[4] The Hong Kong Observatory, Hong Kong, China (email: pwchan@hko.gov.hk)

Abstract

Satellite remote sensing has been extensively utilized for monitoring dust storms in space and time. Dust storm detection using satellite observations is important to analyze the dust storm trajectories and sources. This paper reviews the algorithms for dust storm detection used in multispectral satellite sensors, spanning visible to thermal wavelengths. Four categories of dust detection algorithms are summarized, namely, dust spectral index algorithms, temporal anomalous detection algorithms, spatial coherence tested algorithms (physical-based algorithms) and machine learning-based algorithms. Following discussions of dust storm detection algorithms, the dust presence validation methods are also reviewed. Future developments for dust storm detection are focused upon three aspects: detection of dust storms at nighttime; development of more efficient machine learning methods for retrieval; and integrating physical and machine learning methods for satellite images.

Keywords: dust storm detection; satellite remote sensing; machine learning

1. Introduction

According to the World Meteorological Organization, a dust storm is defined as 'strong winds that lift large quantities of dust particles and reduce visibility to less than 1000 m' (Goudie and Middleton, 2006). Dust storms play a significant role in global climate change and have become a major environmental concern. It also creates substantial adverse impacts on human health and ecosystems, which could result in losses in economy and human life (Ackerman and Chung, 1992; Meskhidze et al., 2005; Slanina, 2007; Weger et al., 2018). Therefore, it is necessary to derive timely and accurate information on dust storms. Satellite remote sensing has been extensively applied to dust storm monitoring due to its distinctive advantages of large coverage and continuous observations. This technique can identify the extent and intensity of dust storms. Dust extent or presence is mainly identified using dust detection algorithms that identify dust pixels on a satellite image.

In recent decades, many dust storm detection methods have been developed. To date, there have only been two studies which reviewed dust storm detection methods (Muhammad et al., 2012; Shao and Dong, 2006). Both papers cover a very wide range of dust storm research, such as dust storm climates, modeling and monitoring (Shao and Dong, 2006), and dust storm detection techniques and technologies (Muhammad et al., 2012). However, in these two review papers, the summary of dust storm detection algorithm is not comprehensive. Moreover, an abundance of new methods has been developed since 2012. These algorithms

were generally classified by spectral range such as visible near-infrared, thermal-infrared, ultraviolet and microwave. Our current study will summarize the algorithms used in dust detection, and new algorithms can also be developed based on the modification of these algorithms for new sensors.

Many satellites or sensors have been applied to dust storm detection along with the development of corresponding methods, such as ultraviolet sensor TOMS, and OMI with the ultraviolet absorption aerosol algorithms (Chiapello et al., 1999; Torres et al., 1998; Torres et al., 2007; Varga et al., 2014), visible to thermal-infrared sensors MODIS, GEOS, AVHRR and dust indices (Ackerman, 1989, 1997; Norton et al., 1980; Prata, 1989; She et al., 2018; Verge-Depre et al., 2006; Wald et al., 1998; William and Robert, 1974), and microwave sensors TRMM, AMSU,AMSR-E, AMSR2 and their polarization indices (El-Askary et al., 2006; El-Askary et al., 2003; Ge et al., 2008; Huang et al., 2007; Kim et al., 2017). Generally, the algorithms developed for the three spectrums using either spectral, spatial or temporal information. One exception in microwave sensors is that polarization information is also used. The most significant drawback of dust storm detection using ultraviolet and microwave sensors is the coarse spatial resolution. Thus, in this paper, we will focus on reviewing the algorithms in the visible to thermal-infrared spectrum. We shall conduct a comprehensive review of dust storm detection algorithms from 1970 to 2020, with representative algorithms being selected and discussed. The algorithms are classified into three categories based on their spectral, temporal, and spatial characteristics.

The paper is structured as follows: Section 2 reviews current multispectral sensors/satellite used for dust storm detection. Then, Section 3 and 4 summarizes current dust storm detection algorithms and dust presence validation data, respectively. Section 5 states the limitations or problems exist in the present dust detection algorithms, and Section 6 presents some future development directions.

2. Satellites and Sensors

Multispectral sensors are mainly onboard two types of satellites, namely polar orbiting satellites and geostationary satellites. The MODIS (Terra & Aqua), AVHRR (NOAA), and MERSI2 (FY-3D) are onboard polar orbiting satellites. The SEVIRI (Meteosat 8-10), GEOS Imager (GEOS 8-15), MTSAT-2 Imager (MTSAT-2), AHI (Himawari 8/9), AGRI (FY-4A), ABI (GEOS 16, 17), AMI (GK-2A) and the future FCI (MTG-I1 to MTG-I4) are onboard geostationary satellites (GEO). The detailed spectral response function (SRF) and spatial resolution information of ten sensors are illustrated in Fig. 1. FCI is excluded because its SRF is not yet available. Polar orbiting satellites provides low temporal resolution but high spatial and spectral resolution for earth observations. Geostationary satellites orbit at high altitude and they remain stationary with reference to the Earth. Thus, sensors onboard GEO observe the Earth in high temporal resolutions (30 min for GEOS and MTSAT, 15 min for SEVIRI and AGRI, 10 min for ABI, AHI, AMI and FCI of full disk) with low spatial and spectral resolution. Geostationary satellites allow continuous observations, hence being capable of monitoring the formation and transportation of dust storms.

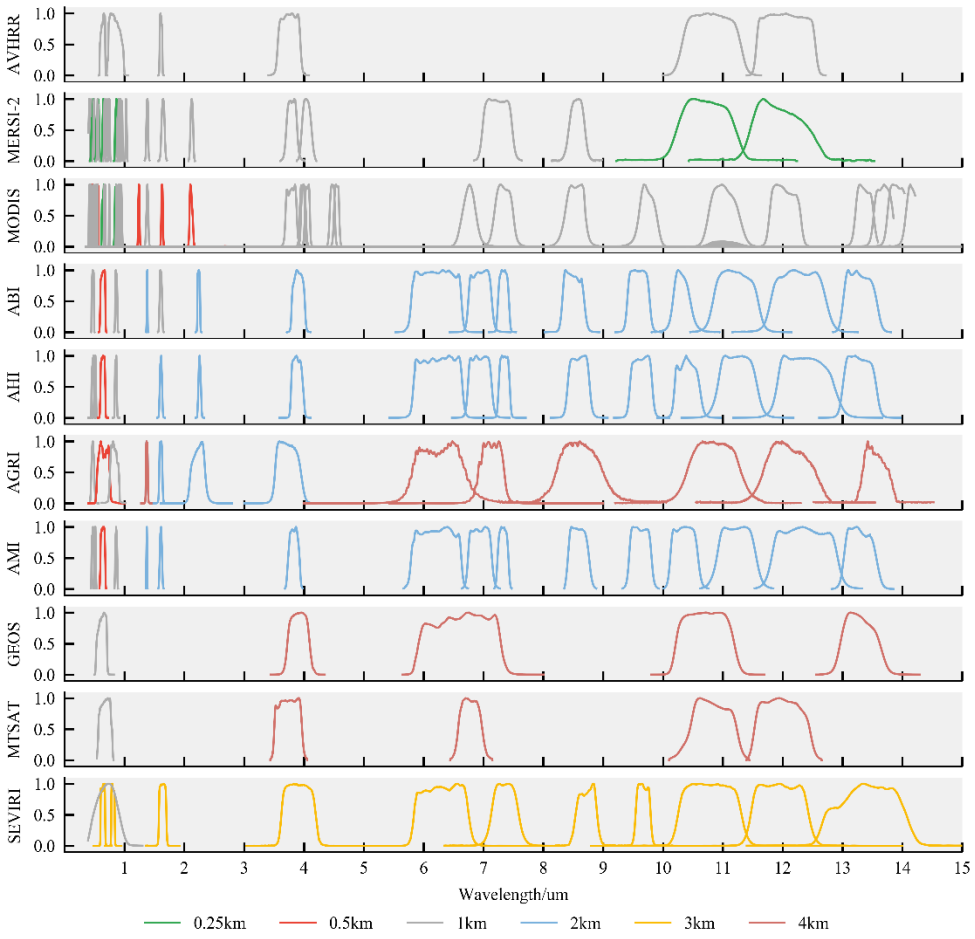

Fig. 1. Spectral Response Function and spatial resolution of commonly used optical sensors for dust detection

MODIS has been extensively used in dust storm studies in previous decades because of its higher spatial resolution and spectral resolution (Baddock et al., 2009; Butt and Mashat, 2018b; Filonchyk et al., 2018; Kazi A et al., 2018; Liu et al., 2013; Park et al., 2014; Prachi and Pravin, 2014; Roskovensky and Liou, 2005; Samadi et al., 2014; Su et al., 2017; Xu et al., 2011a; Yue et al., 2017; Zhao et al., 2010). However, dust storms have a short lifetime (sometimes even last within hours) but large spatial coverage. Thus, geostationary satellites are capable of capturing the temporal variations of dust storms; especially in recent years, when the new generation of geostationary satellites have been launched with more channels, and improved spatial and temporal resolution (e.g., Fengyun-4A, Himawari8/9, GEOS16/17, GEO-KOMPSAT-2A). This type of satellites is mainly used for meteorological applications (Ashpole and Washington, 2012; Cecchi et al., 1998; Evan et al., 2006; Hong, 2009; Hu et al., 2008; Legrand et al., 2001; Sannazzaro et al., 2014; She et al., 2018; Tramutoli, 2007; Tramutoli et al., 2010; Verge-Depre et al., 2006).

3. Dust Detection Algorithms

In medium spatial resolution satellite images, dust contaminated pixels need to be distinguished from cloud pixels, dark land surface pixels, bright land surface pixels, and water surface pixels. As distinguished by Shahrisvand and Akhoondzadeh (2013), there are basically two methods for dust detection: empirical physical-based, and machine learning-based methods. The empirical methods are physical, radiance-based approaches that depend on the physical properties and spectral signature of dust particles in the visible, near-infrared and thermal bands (Yan et al., 2020). Physical-based algorithms are more mature in their state of development and are commonly used. However, this type of method is limited by their dependence on

thresholds which can be a function of land cover types, dust aerosol properties and illumination geometries. The machine learning-based approach is more flexible, and does not require a presumed threshold, but it may be complex in structure design of some ML algorithm, such as maximum likelihood classification (MLA), support vector machine (SVM) and artificial neural network (ANN). Both physical-based and machine learning-based methods will be reviewed in this paper.

Physical-based methods utilize the spectral, spatial and temporal information to distinguish dust from cloud and clear-day surface. The reflectance of dust storms is often greater than that of clear-day land or water surface, while dust storm temperature is often cooler than the underlying surface. The spectral signature of dust is thus distinctive from surface and cloud. Dust storms also tend to be more homogeneous than the underlying land surfaces in both visible near-infrared (VIR) and thermal infrared (TIR) images. These properties have been utilized to develop a variety of threshold test to distinguish dust from clear-day surfaces and clouds. The threshold value, in general, is determined using histograms or scatterplots of the samples from satellite observations. According to these properties, physical-based dust detection algorithms can be further classified into three categories based on different information used, namely, spectral index algorithm, temporal anomalous algorithm, and spatial coherence test algorithm. The details of these algorithms will be discussed in the following sections. We will only briefly summarize the machine learning algorithms being used in the present literature, whereas in-depth discussion of machine learning algorithms is beyond the scope of this paper.

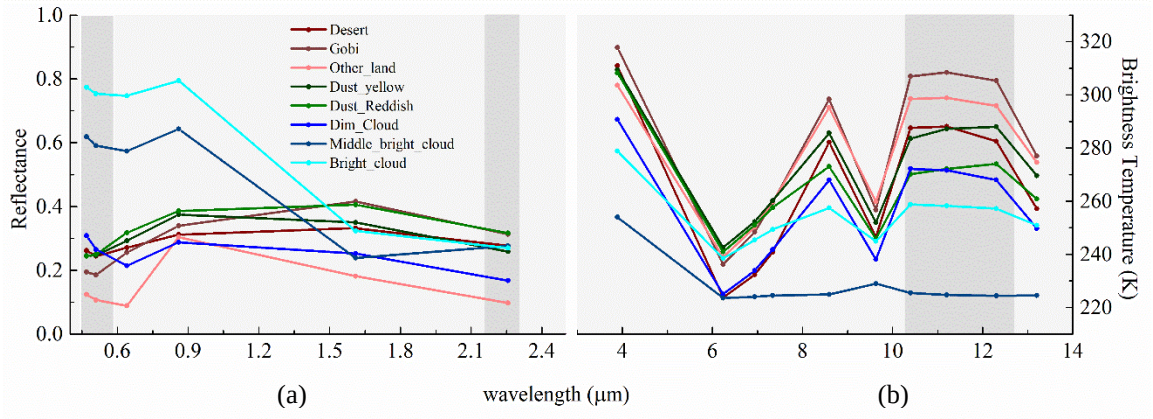

Fig. 2. Spectral signature of different features at (a) visible near-infrared channels and (b) thermal-infrared channels. The spectral signature curves of the eight features are sampled from AHI (onboard Himawari satellite) observations.

3.1. Dust Spectral Index Method

The Dust Spectral Index Method utilizes the spectral signature of dust storms. Different features have different spectral signatures that describe their absorption and scattering ability at different wavelengths. Three major features can be visually distinguished from medium spatial resolution (e.g. 0.5 km ~ 1 km for MODIS) images: clear-sky surface (land, ocean), clouds and aerosols (e.g. dust storm, volcanic ash, smoke). The dust indices separate different features by expressing the major differences in the spectral signature of features in both solar reflectance bands and infrared emissivity bands. We take samples of eight features from AHI (Advanced Himawari Imager) observations to illustrate spectral signature of different features (Fig. 2 (a) and (b), respectively). Fig. 2(a) shows that clouds generally have high reflectance in the visible bands and low reflectance in the near-infrared bands, but dust generally shows low reflectance at visible bands but high reflectance in the near-infrared bands. Fig. 2(b) shows that in the thermal spectrum spanning from 10 μm to 12 μm, dust exhibits an increasing brightness temperature, while clouds and other background features exhibit decreasing brightness temperatures. The brightness temperature difference (BTD) (Ackerman, 1997; Prata, 1989) and Normalized Dust Difference Index (NDDI) (Qu et al., 2006) are two major dust detection algorithms that utilize the spectral signature in the thermal and visible to near-infrared regions, respectively. Enhanced methods are developed to employ the merits of BTDs and NDDI including the Brightness

Temperature Adjusted Dust Index (BADI) (Yue et al., 2017); Three-band Volcanic Ash Product (TVAP) (Ellrod et al., 2003); Normalized Dust Layer Index (NDLI) (Kazi A et al., 2019). Other dust indices include the Thermal-infrared Dust Index (TDI) (Hao and Qu, 2007), MEDI (Karimi et al., 2012), and D-parameter (Roskovensky and Liou, 2003). These indices are constructed using the sensitive channels to dust, which are wavelengths around 0.65, 0.86, 2.3, 3.7, 8.6, 9.6, 11, and 12μm. Most of these indices only use the thermal bands except the D-parameter, which uses both thermal and visible bands. The BTD_{i-j}, BT_i and R_i in the following sections stand for BTD between band i and band j, brightness temperature at band i and reflectance at band i, respectively.

3.1.1. Brightness Temperature Difference

The BTD technique (or split window technique) is the most widely used technique. It utilizes the unique spectral signature of dust in the TIR region. Silicate exhibits a "V" shape in the spectral region from 8.3 μm to 12.0 μm, and it composes a large part of dust. This technique was primarily developed for volcanic aerosol detection (Prata, 1989) which utilizes the BTD of 11 μm and 12 μm. It was later applied for dust detection due to the similarities between mineral dust aerosol and volcanic aerosol (i.e. the silicate component is contaminated by both dust and volcanic ash). The BTD technique is based on the principle that dust particles extinct more radiation at 11 μm than 12 μm while reverse effect observed for cloud, leading a negative value of $BTD_{11\text{-}12}$ for dust and positive value for cloud (Potts, 1993; Prata, 1989). BT_{11} further decreases as dust layer rises, thus, results in more negative $BTD_{11\text{-}12}$. Generally, $BTD_{11\text{-}12}$ is sensitive to high-density and high-altitude dust storms which can lead to more negative $BTD_{11\text{-}12}$, while being less sensitive to low-density or low-altitude dust cases (Kazi A et al., 2019). $BTD_{11\text{-}12}$ is near zero for most underlying surfaces (except for bright surfaces, e.g., deserts). Despite the simplicity, the magnitude and sign of BTD are not only determined by dust mineral composition, dust optical thickness, dust layer altitude, but they also vary with the surface emissivity and view zenith angle (Bin Abdulwahed et al., 2019). A dust/non-dust threshold of zero for $BTD_{11\text{-}12}$ is not explicitly presented. However, negative differences in $BTD_{11\text{-}12}$ for dust storms were observed, implying a universal threshold of $BTD_{11\text{-}12} < 0$ for dust (Ackerman, 1997). Darmenov and Sokolik (2005) found the thresholds of BTD can be set as 0.5, -0.2, -1.0, -0.4 K for Gobi/Taklimakan desert, Australian desert, Nubian, and Thar desert. It is impossible to determine a definite threshold for the universal applications.

The brightness temperature difference at 3.7 μm and 11 μm was also applied to dust storm detection, according to the principle that the BTD of dust between 3.7 and 11 μm was enhanced by a dust reflection of 3.7 μm solar radiation (Ackerman, 1989). $BTD_{3\text{-}11}$ is sensitive to dust loading and thus also feasible for AOT retrieval. In addition, $BTD_{11\text{-}12}$ alone may misclassify bright surfaces (e.g., deserts, arid, or semi-arid regions) as dust storms, when combined with $BTD_{8\text{-}11}$, it can identify dust more robustly (Ackerman, 1997) as $BTD_{8\text{-}11}$ is sensitive to dust loading over sandy surfaces, and is insensitive to dust height (Wald et al., 1998). Larger amounts of airborne dust indicate more negative values of $BTD_{8\text{-}11}$. These above mentioned BTD algorithms are denoted with the following functions:

$$BTD_{11-12} = BT_{\sim 11.2} - BT_{\sim 12.4} \quad (3\text{-}1)$$

$$BTD_{3-11} = BT_{\sim 3.9} - BT_{\sim 11.2} \quad (3\text{-}2)$$

$$BTD_{8-11} = BT_{\sim 8.6} - BT_{\sim 11.2} \quad (3\text{-}3)$$

Although the BTD technique is effective, there are still some limitations (Prata et al., 2001). Negative $BTD_{11\text{-}12}$ could be caused by strong surface-based temperature inversions, barren surfaces such as deserts, volcanic ash and clouds over the tropopause, instrument noise and channel misregistration. Thick dust storms appear to have positive $BTD_{11\text{-}12}$ values, and high-water burdens (such as over tropical area or ocean) could also mask the negative $BTD_{11\text{-}12}$ when viewing an actual dust cloud, which most often occurs in the tropics (Prata et al., 2001).

3.1.2. Normalized Difference Dust Index

Another classic dust index is the NDDI, which uses the spectral characteristics in the visible (near 0.469 µm) and near-infrared bands (near 2.13 µm) (Qu et al., 2006). This algorithm is expressed as follows:

$$NDDI = \frac{\rho_{2.3\mu m} - \rho_{0.47\mu m}}{\rho_{2.3\mu m} - \rho_{0.47\mu m}} \quad (3\text{-}4)$$

The Advanced Spaceborne Thermal Emission and Reflection Radiometer (ASTER) spectrum library is utilized by Qu et al. (2006) to analyze the spectral signature of seven features. Over visible to near-infrared spectrum (i.e., 0.4 to 2.5 µm), the spectral signature of dust in the reflectance spectrum generally shows an increasing pattern, peaking at ~2.13 µm; whereas cloud shows the opposite trend with the highest point at ~0.469 µm and the lowest point at ~2.13 µm. Therefore, NDDI is generally positive for dust pixels, negative for clouds, and near-zero for clear-sky surface. This indicates that NDDI can distinguish dust storms from clouds. However, the NDDI is neither sensitive to dust density nor dust altitude, thereby shows low values even at high-density dust storm. It is also deficient over bright surfaces as they show similar spectral pattern with dust spanning visible to near-infrared spectrum. Therefore, NDDI has difficulty in distinguishing dust from these bright surfaces (Qu et al., 2006; Xu et al., 2011b). NDDI is generally used to detect dust along with BTD, which can eliminate ground surface (Kazi A et al., 2019; Xu et al., 2011b).

3.1.3. Thermal Infrared Dust Index

The TDI algorithm utilizes four MODIS thermal bands to detect dust (Hao and Qu, 2007). This algorithm has potential for nighttime dust detection and indication of dust density, as it can derive the index for AOT at 550 nm. TDI can be used as a proxy variable for estimating dust intensity, and allows for the separation of Sahara dust storms from background aerosols. This algorithm is denoted as follows:

$$TDI = C_0 + C_1 \times BT_{3.7} + C_2 \times BT_{9.7} + C_3 \times BT_{11} + C_4 \times BT_{12} \quad (3\text{-}5)$$

Where the coefficients C_0, C_1, C_2, C_3 and C_4 are set as -7.937, 0.1227, 0.0260, -0.7068 and 0.5883 respectively (Hao and Qu, 2007). Coefficients are estimated by constructing regression relationship between AOD and BTs. Effectively, TDI is the weighted summary of the four BTs with the largest weight on BT11 and then follows with BT_{12} and $BT_{3.7}$. $BT_{9.7}$ gets the least weight in TDI which is rarely used for constructing dust index as it is also sensitive to ozone (Coheur et al., 2005; Landgraf and Hasekamp, 2007). The TDI can detect dust during both day and night, as it uses only the thermal wavelengths, but it can only be applied over oceans.

3.1.4. Middle East Dust Index (MEDI)

The MEDI combines wavelength at around 8.55, 11 and 12 µm to distinguish between dust and desert surfaces (Karimi et al., 2012) and was designed specifically for dust detection over Middle East areas. The MEDI can identify dust plumes, dust sources and desert surfaces, and is defined as follows:

$$\text{MEDI} = \frac{BT_{11} - BT_{8.5}}{BT_{12} - BT_{8.5}} \quad (3\text{-}6)$$

MEDI values greater than 0.6 indicates being dust-contaminated. The main challenge for dust detection is misclassifying desert surfaces as dust pixels (Ackerman, 1997; Roskovensky and Liou, 2005). The MEDI is designed to address this problem and it has been shown to be capable of separating dust from desert surfaces (Karimi et al., 2012).

3.1.5. Three-band Volcanic Ash Product

TVAP was originally developed for volcanic ash detection (Ellrod et al., 2003). It integrates $BTD_{12\text{-}11}$ and $BTD_{3\text{-}11}$, therefore being able to indicate both dust presence and dust intensity. This technique calculates the sum of two BTDs by assigning different weights to these BTDs. The TVAP is defined as follows:

$$\mathrm{TVAP} = 60 + 10(BT_{12.4} - BT_{11.2}) + 3(BT_{3.9} - BT_{11.2}) \quad (3\text{-}7)$$

At daytime, the brightness temperature near 3.7 μm contains both solar reflectance and terrestrial emission. At night, reflective component weakens, so the emissivity and transmittance characteristics dominates. Such characteristics lead to pronounced diurnal variations of $BT_{3.7}$, and further derivation of TVAP. Therefore, specific thresholds of TVAP that distinguish dust storms and non-dust features should be established on a case-by-case basis.

3.1.6. Brightness temperature Adjusted Difference Index

The BADI enhances BTD methods by synthesizing two BTDs ($BTD_{3\text{-}11}$ and $BTD_{11\text{-}12}$) (Yue et al., 2017) based on the principle that $BTD_{11\text{-}12}$ can be used to detect the dust extent, and $BTD_{3\text{-}11}$ can indicate dust density. A higher $BTD_{3\text{-}11}$ value indicates a higher dust density. Thus, the BADI can simultaneously detect dust storm extent and density. Several dust storms that occurred between year 2000 and 2011 over northeast Asia were used to test this algorithm, and the results were compared to the existing dust indices, such as the $BTD_{11\text{-}12}$ and NDDI (Yue et al., 2017). The comparison results showed that BADI performs better in capturing the spatial extent and density of dust storms.

$$\mathrm{BADI} = \frac{2}{\pi} \times \arctan\left(\frac{\mathrm{BDI}}{BDI_{0.95}}\right) \quad (3\text{-}8)$$

where BDI= $(BTD_{3.9-11.2})^2 \times BTD_{12.4-11.2}$.

3.1.7. D-parameter algorithms

The P-parameter index was first developed to detect thin cirrus clouds, by combing the ratio ($R_{1.38}/R_{0.65}$) and $BTD_{8\text{-}11}$ (Roskovensky and Liou, 2003). The D-parameter index was then developed to further separate dust storms from cirrus clouds by combining the distinct features at both visible to near-infrared spectrum and thermal spectrum (Roskovensky and Liou, 2005). The D-parameter integrates the $BTD_{11\text{-}12}$ with a reflectance ratio ($R_{0.54}/R_{0.86}$). Pixels where the D-parameters are greater than 1.0 are defined as dust-contaminated. The combination of the D-parameter and P-parameter is genuinely robust enough to accurately distinguish dust from cirrus clouds on satellite images (Roskovensky and Liou, 2005). The P-parameter and D-parameter are expressed as follows:

$$\mathrm{P-parameter} = \exp\left(-\left(\frac{R_{1.38}}{R_{0.65}} + \left(T_{B,8.6} - T_{B,11}\right) - \mathrm{b}\right)\right) \quad (3\text{-}9)$$

$$\mathrm{D-parameter} = \exp\left(-\left(\frac{R_{0.54}}{R_{0.86}} + \left(T_{B,11} - T_{B,12}\right) - \mathrm{b}\right)\right) \quad (3\text{-}10)$$

Dust indices are simple and efficient in most cases. However, there is evidence suggesting that dust properties vary significantly among dust sources. Darmenov and Sokolik (2005) demonstrated that mineralogical composition is a crucial factor affecting the radiative properties of dust and suggested variable dust thresholds which can be comprehensively determined by dust loading, dust mineralogical composition, dust vertical distribution, and dust size.

3.2. The anomalous dust detection method

Disturbances such as cloud, smoke, biomass burning, hurricane and land cover change can be well-detected by anomalous detection methods. Generally, the anomaly caused by cloud disturbance is the largest, followed by natural disasters such as dust storms, volcanic eruptions, hurricanes, and natural land cover changes. By defining different thresholds, a dust storm can be differentiated from clouds as well as clear-sky surfaces in a very general way. Normally, this type of algorithms should be combined with other detection algorithms for dust detection.

The anomalous detection algorithms use time series images that capture the scene at the same location and time period. The algorithm assumes a steady Earth-atmosphere system (i.e. the water vapor effect is not considered). Therefore, anomalies appearing on the observation images are likely to be caused by the presence of a variable atmosphere, owing to cloudiness, dust storms, or other natural hazards. The anomalous algorithms can be applied to any wavelengths and any indices which are sensitive to dust storms. The representative anomalous dust detection algorithms are as follows:

- The Infrared Difference Dust Index (IDDI) (Legrand et al., 2001) uses the brightness temperature depression at 11 μm:
- $$IDDI = BT_{ref} - BT \quad (3\text{-}11)$$
- The Minimum Reflectance (MR) developed by Herman and Celarier (1997) which uses ultraviolet bands, and then modified by (Wong et al., 2011), which uses the reflectance increment in the visible band:
$$Min_{Ref} = \mathrm{R} - R_{ref} \quad (3\text{-}12)$$
- The BTD anomalous BTD_{anom} (Ashpole and Washington, 2012) and the Dynamic Reference brightness temperature difference DRBTD (Liu et al., 2013), both uses the deviation of dust BTD from reference BTD (or surface BTD). Large deviation of BTD indicates high possibility of dust.
- The Robust Satellite Technique (RST) performs robustly and can be extended to different geographical and seasonal conditions (Cecchi et al., 1998; Sannazzaro et al., 2014; Tramutoli, 2007; Tramutoli et al., 2010).

Although both BTD_{anom} and DRBTD use the BTD anomaly information, the BTD_{anom} composites the reference image by calculating the mean BTD values from previous data under cloud and dust-free conditions, while DRBTD composites the reference image by establishing the relationship between BT11 and BTD under clear conditions. The RST is more complex and more robust. This algorithm differs from other anomalous detection algorithms by incorporating a normalization process using standard deviation.

Temporal anomalous dust detection algorithms are generally used by sensors aboard geostationary satellites, because of their fixed observation areas and high temporal resolution. Some sensors aboard polar orbiting satellites can also use this algorithm, but only by registering and rectifying the time series images in advance. These types of algorithms are very efficient due to their high sensitivity. However, the disadvantage is that some anomalies that are not of interest, such as land cover changes and temperature changes, may also be detected.

3.3. Spatial coherence test method

Since heavy dust storms and thin clouds such as cirrus have very similar spectral signature, algorithms based on spectral information may have difficulties separating clouds and heavy dust storms (Martins et al., 2002). Scene uniformity can be used as a tool for discriminating heavy dust storms from clouds, especially cirrus or cloud edges. Clouds show a highly heterogeneous spatial structure, while aerosols show a highly uniform spatial structure on the scale from a hundred meters to a few kilometers (Coakley and Bretherton, 1982). The spatial coherence test method is based on this physical difference. Spatial coherence test also known as spatial variability test or uniformity test is normally represented by standard deviation.

Generally, a 3 × 3 standard deviation (3×3-STD) algorithm is used as a spatial coherence test. High STD values normally indicate clouds, while low STD values can be represented by aerosols or clear sky (Martins et al., 2002). A spatial coherence test was originally conducted with infrared bands (11 μm) for cloud masking (Coakley and Bretherton, 1982). A similar method was later applied to separate dust from clear-sky surfaces and clouds using Meteosat images (Jankowiak and Tanré, 1992). A 3×3-STD at infrared can be applicable for cloud masking at both daytime and nighttime. However, it could work in visible wavelengths and may not be very sensitive to spatial variability in near-infrared wavelengths. Martins et al. (2002) found that over ocean, a 3×3-STD at 0.55 μm is most suitable to distinguish aerosols and clear area from cloud. Most cloud contaminated pixels can be screened out by the 3×3-STD with a constrained and a relaxed threshold of 0.0025 and 0.038 respectively. However, a 3×3-STD at 0.47 μm may not be applicable over ocean because of its high reflectance of ocean and large variability caused by chlorophyll. Zhao et al. (2010) applied a 3×3-STD at 0.86 μm to detect dust and smoke over ocean and applied a 3×3-STD at 0.64 μm to detect smoke over land, therein $STD_{0.86}$ less than 0.005 being dust or smoke and $STD_{0.64}$ less than 0.04 being smoke over ocean.

The spatial coherence test has advantages of being simple, less influenced by calibration errors, being not strongly dependent on wavelength, easily transferrable to other sensors. Spatial coherence test is mainly used to screen out clouds which have similar spectral properties as dusts. It has been demonstrated to be effective for discriminating homogeneous dust layers from heterogeneous clouds, especially over oceans. However, this type of methods can only be used along with spectral index method and anomalous detection method.

3.4. Machine learning-based algorithms

Machine learning-based methods are data-driven methods, which can detect dust presence by self-learning from the given training dataset. The main limitation of physical threshold-based methods is the threshold determination, which has high variation in respect to the variation of land covers (Rivas-Perea et al., 2010a). Machine learning-based methods can overcome this limitation, and have proven to be useful for dust storm detection (Shi et al., 2019; Shi et al., 2018). Physical-based dust detection methods are relatively mature, while the Machine learning-based methods still require more study. There are three aspects that need to be carefully considered when using machine learning-based methods. These include input data, data for labeling, and machine learning algorithms. Input data are mainly from satellite observation data, including reflectance, brightness temperature, satellite illumination and observation geometries, and dust indices. Some literature also used ancillary data as input, such as land surface type and altitude. The input data need to be carefully selected, and redundant features should be deleted to avoid decrease in prediction accuracy. An independent set of data should be used for labeling which shows whether a pixel is dust contaminated or not. This set of data can be obtained from manual interpretation (Rivas-Perea et al., 2010a). Rivas-Perea et al. (2010a) manually classified dust pixels into dust storm, blowing dust, smoke and background. It can also be determined from MODIS AOT, CALIPSO VFM, OMI AI and AAOT, and AERONET AOT and angstrom exponent products. The labeled data is also used as the validation data, and the detailed discussion of validation dataset can be found in Section 4. As for training algorithms, several machine learnings used for classification and regression are applicable for dust storm detection. Generally, the Maximum Likelihood classifier (ML), Logistic Regression (LR), Support Vector Machine (SVM), Random Forest (RF), Artificial Neural Network (ANN) and Probabilistic Neural Network (PNN), have been applied for dust storm detection (Rivas-Perea et al., 2010a; Rivas-Perea et al., 2013; Rivas-Perea et al., 2010b; Shahrisvand and Akhoondzadeh, 2013; Shi et al., 2019; Shi et al., 2018; Souri and Vajedian, 2015). The machine learning algorithms are inter-compared. Rivas-Perea et al. (2010b) indicated improved classification performance of PNN than ML classifier. Shahrisvand and Akhoondzadeh (2013) stated that SVM performed better than decision tree and ANN. Rivas-Perea et al. (2013) showed SVR outperforms other neural network-based classifier. Machine learning algorithms used in dust detection need to be carefully selected and compared. Ensemble methods are also recommended to combine several machine learning results to strengthen the weak predictors.

3.5. Comparison between different methods

Four types of dust detection methods discussed above have their own merits and limitations. The three physical-based methods are complementary to each other. Most of the dust storm or dust plume pixels can be detected with spectral index method. BTD algorithms especially $BTD_{11\text{-}12}$ are very effective and has been widely used in all kinds of situations. At visible to near-infrared (VIR) spectrum, NDDI as the most representative algorithm, is effective to distinguish dust from clouds. The concept of other ratio algorithms is similar with NDDI which also take advantage of the spectral difference between dusts and clouds in visible to near-infrared spectrum. Both BTD and NDDI are available for most of multispectral sensors. With simple mathematical calculations, this type of algorithms is able to detect most of dust pixels. It is simple, effective, efficient and can be applied to sensors onboard both geostationary and polar orbiting satellite. Temporal anomalies and spatial coherence test method are not suggested to be solely used in the dust detection. Dust spectral index mainly utilizes the spectral pattern of dust to distinguish it from other features, thereby being unable to cope with features having similar spectral patterns with dusts, e.g., desert or arid surface. Temporal anomalies algorithms can handle these situations by compositing a reference image as the background image or clear-sky image from time-series images. This type of algorithms requires a period (e.g. 15, 30 or 60 days) of time-series images which capture sceneries at same location, therefore it is more applicable to geostationary satellites. This method may not be worked if there is no clear day, or the surface temperature/reflectance has large variations during the period of time. Spatial coherence test is mainly used to screen out clouds which have similar spectral properties as dusts. It has been demonstrated to be effective in discriminating homogeneous dust layers from heterogeneous clouds, especially over oceans. This type of algorithms is less influenced by calibration errors and not strongly dependent on wavelength thus can being easily transferrable to other sensors. Both temporal anomalies detection and spatial coherence test methods are not capable of accurately detecting dust pixels by their own but could be incorporated along with spectral index algorithms. From the above discussion, it can be noticed that for physical-based methods, accurate dust detection requires considering all the three methods since they are capable of tackling different dust detection issues. Moreover, existing physical-based methods are generally threshold-based which are of great complexity and uncertainty, since different sensors, backgrounds, dust aerosol properties can lead to large threshold variances. Machine learning method is more and more preferable by researchers in remote sensing discipline. This method is data-driven and do not require the pre-requisite of threshold setting. It learns from classification rules from a given dataset and can integrate data from different sensors for retrieving information. However, this type of method is highly depended on its training dataset. If the training dataset is biased, the classification results are likely to be biased as well. Table 1 summarizes four methods with representative algorithms, references and application scenarios. Although the algorithms listed in this table focused on dust storm detection, some of the algorithms are not originally designed for but are later introduced into dust storm detection (e.g., TVAP, Min_Ref, STDs).

Table 1. Summary of dust detection algorithms.

Algorithm type	**Algorithm name**	**Application scenarios**	**Reference**
Dust spectral index	$BTD_{11\text{-}12}$	the most effective algorithm under most situations but shows limited ability over desert surfaces	(Ackerman, 1997)
	$BTD_{3\text{-}11}$	effective at daytime and having the potential to infer optical depth of dust	(Ackerman, 1989)
	$BTD_{8\text{-}11}$	sensitive to dust loading over desert background and insensitive to dust height	(Ackerman, 1997; Wald et al., 1998)
	NDDI	effective to distinguish dust pixels from cloud pixels	(Qu et al., 2006)
	TVAP	sensitive to both dust presence and intensity	(Ellrod et al., 2003)
	BADI	same as TVAP	Yue et al. (2017)
	NDLI	being able to indicate the phase (e.g. originating, blowing) of dust storm	(Kazi A et al., 2019)

	TDI	being sensitive to dust intensity	(Hao and Qu, 2007)
	MEDI	effective over desert surfaces, especially Middle East	(Karimi et al., 2012)
	D_parameters	accurately distinguish dust from cirrus	(Roskovensky and Liou, 2005)
Temporal anomalous detection	IDDI	effective over desert	(Legrand et al., 2001)
	Min_Ref	effective over surfaces having large color contrast with dust storm (e.g. ocean, vegetated area)	(Herman and Celarier, 1997; Wong et al., 2011)
	RST	performs well over all situations but is more effective with geostationary satellite data	(Cecchi et al., 1998; Tramutoli et al., 2010)
	BTDanom	same with RST	(Ashpole and Washington, 2012)
	DRBTD	same with RST	(Liu et al., 2013)
Spatial coherence test	STD_11μm	being able to distinguish dust from cloud at both day and night detection	(Coakley and Bretherton, 1982)
	STD_0.55μm	being able to distinguish dust from cloud over ocean	(Martins et al., 2002)
	STD_0.86 μm	same as STD_0.55μm	(Zhao et al., 2010)
	STD_0.64 μm	being able to distinguish dust from smoke over land	(Zhao et al., 2010)
Machine-learning based	LR	being able to handle complex situations but being largely dependent on training dataset	(Shi et al., 2018)
	SVR		(Rivas-Perea et al., 2013)
	SVM		(Shi et al., 2019)
	ML		(Rivas-Perea et al., 2010b)
	RF		(Souri and Vajedian, 2015)
	ANN		(Shi et al., 2018)
	PNN		(Rivas-Perea et al., 2010b)

4. Validation of dust presence

Validating dust presence results requires reference data of dust presence. The reference data are also used as labeling data in machine learning-based method. The dust storm detection results can be assessed visually (Miller et al., 2017; Xie et al., 2017; Yan et al., 2020; Yue et al., 2017), and validated against MODIS AOD products (Yan et al., 2020; Yue et al., 2017), OMI Ultra Violet Aerosol Index (UVAI) (Xie et al., 2017), CALIPSO dust type (Prachi and Pravin, 2014; Shi et al., 2018; Xie et al., 2017), AERONET products (Bin Abdulwahed et al., 2018; Butt and Mashat, 2018a), or local meteorological station-based observation using visibility data (Albugami et al., 2018; Butt and Mashat, 2018a; Miller et al., 2017; Samadi et al., 2014; Taghavi et al., 2017).

True-color image comparison through visual assessment is a qualitative validation method. The location of dust events can be clearly seen on true color image. Manual selection of dust storm area by experts from the true-color image can also be used for quantitative validation. The other four validation data types can all be used as quantitative validation. MODIS AOD products can be used to indicate dust presence. Considering that dust aerosol is normally over bright surfaces, the MODIS Deep Blue along with Dart Target (DTB) AOD product is adopted. The OMI onboard Aura is a hyperspectral sensor which can capture signals in the ultraviolet to visible spectrum at a spatial resolution of 13 km × 24 km. It is originally designed for ozone

and other atmospheric components monitoring, and later applied to the discrimination of absorbing (dust, smoke) and non-absorbing aerosols by utilizing Absorbing Aerosol Optical Depth (AAOD) and Aerosol Index (AI). Specifically, high AAOD explains high possibility of dust presence and positive AI generally represents absorbing aerosols (e.g., dust aerosols) with non-absorbing aerosols (e.g., clouds) being negative. The OMI products (OMAERUV AAOD and AI) can be download at Goddard Earth Sciences Data and Information Services Center (https://ssw.gsfc.nasa.gov/SSW/). Park et al. (2014) determined dust pixels by using AAOD > 0.4 and AI > 0.7. The low spatial resolution can be one of the limitations in OMI AAOD for validation. AERONET is a global aerosol observation network which measures radiance at eight wavelengths (340, 380, 440, 500, 675, 870, 940 and 1020 nm). It provides aerosol property products including AOT, angstrom exponent (α), aerosol size distribution, single scattering albedo, asymmetry factor, and complex refractive index. These data are freely accessible at NASA's AERONET website (https://aeronet.gsfc.nasa.gov/). Dust and non-dust can be coarsely separated with angstrom exponent. The value of angstrom exponent less than 1 indicates a dominance of coarse mode aerosols such as dust and sea salt (Marchese et al., 2017; Schuster et al., 2006). AERONET sites are sparsely distributed, and thus can only provide point data for validation. CALIOP onboard CALIPSO is a two-wavelength (532nm and 1064nm) polarization Lidar designed to measure aerosol vertical profiles. The CALIPSO footprint, overlaying the multispectral sensor observation scene, can be used as validation. The CALIPSO product Vertical Feature Mask (VFM) provides aerosol type information, which classifies the aerosol into clean marine, dust, polluted continental/smoke, clean continental, polluted dust, elevated smoke and dusty marine (Man-Hae et al., 2018) where dust, polluted dust and dusty marine aerosols are clustered as dust and other types as non-dust (Shi et al., 2018). The CALIPSO VFM product description can be found in the NASA CALIPSO website (https://www-calipso.larc.nasa.gov/) and the data are accessible at the website of Earthdata Search (https://search.earthdata.nasa.gov/search). The CALIPSO product can offer more precise dust information by utilizing its vertical profile but it is extremely limited by its narrow swath measurement, i.e. validating limited dust pixels along its strip-shape footprints.

5. Limitations in the existing dust detection algorithms

There are five issues that pose difficulty in implementing physical-based algorithms. First, most dust detection indices are not applicable over bright surfaces (e.g., desert and barren lands). These bright surfaces, especially desert surfaces, have similar spectral signature as dust storm. Second, thresholds of dust indices can be highly variable. The thresholds of dust detection indices can be influenced by dust properties (e.g., optical thickness, particle size, complex refractive index), dust layer height, and land cover type (Darmenov and Sokolik, 2005). Spectral signature of different sensors can also result in threshold difference for the same dust indices. Take BTD_{11_12} as an example, the center wavelength of the two thermal channels are 11 and 12 μm for MODIS, 10.8 and 12 μm for AVHRR and MTSAT, 11.2 and 12.4 μm for AHI. Detailed Spectral Response Function (SRF) of commonly used sensors can be referred to Fig. 1. Incorrect threshold value could result in large, undetected or falsely detected dust pixels. Therefore, case-by-case determination of thresholds are necessary. Third, cirrus have similar characteristics as dust storm; thus, cirrus can be easily interpreted as dust. Fourth, nighttime dust detection can be difficult in terms of less information and reduced spectral difference. Reflectance at visible to near-infrared wavelength is no longer available and only brightness temperatures can be obtained at thermal wavelength. Besides as surface temperature cools down, the brightness temperature difference between clear-day surface and dust are significantly reduced. Fifth, water vapor can mask the dust signals. Especially in tropical areas, water absorbs more radiation at 12 μm than 11 μm, i.e., $BTD_{11\text{-}12}$ being positive over areas with high density of water vapor. Such characteristics can definitely mask the negative BTD value of dust.

Apart from five issues mentioned above, definite separation of dust storm, clear sky and cloud can be unrealistic. Ambiguity is likely to occur when the value of a dust index is around and close to the threshold values. It is impractical to classify pixels as dust-contaminated, cloud-contaminated, clear-sky definitely, because in nature the optical thickness of dust storm varies continuously in space with a vague margin. Especially, dust storms are often found to swirl with clouds. The cloud contamination in dust pixels could result in errors (generally increasing the AOT value). Depending on the application scenario, the thresholds of dust index can be relaxed or constrained to incorporate more dust-like pixels or to purify the dust category with the identified dust pixels in high confidence.

6. Future development and perspective

Present dust detection literature mainly uses polar orbiting satellite (such as MODIS) for dust storm detection, since these are sun-synchronous, thereby, detecting dust storms mainly during daytime. With the launch of the new generation geostationary satellites, more attention will be paid on GEOs as it can offer continuous earth observation as well as higher resolution (compared with old generation GEOs). Theoretically, present infrared-based dust detection algorithms can be applied to dust storm detection at night, but it is impractical to obtain accurate dust presence product. First, the low surface temperature at night can weaken the dust signal, thus, decreasing the signal-to-noise ratio (SNR) and making the detection difficult. Second, very few validation datasets are available at night. Therefore, dust storm detection at sunset, dawn and nighttime requires more attention and consideration. This issue can be tackled by incorporating useful information from multiple sensors, and this leads to a call for data combination. Machine learning-based method is good at fusing data from different data sources by simply taking them as input data. Additional data such as wind speed could also have an impact on dust storm formation and deposition, and may also be considered in the input dataset (Yan et al., 2020). However, more features do not always lead to higher classification accuracy as redundancy and noise can also be leveled up. Only with more informative features can we generate more trustworthy detection results. For machine learning-based methods, both input features and training algorithms require more consideration. Machine learning methods in computer science are currently undergoing rapid development, and thus more machine learning methods for dust detection may be introduced in the future. Integration of physical-based and machine learning-based methods to improve detection accuracy may be another way forward in the future.

Acknowledgements

This study was supported by the General Research Fund (project ID: 15205515) and Collaborative Research Fund (project ID: C7064-18GF) from the Research Grants Council of Hong Kong. The authors thank the Meteorological Satellite Centre of Japan Meteorological Agency for providing AHI image data.

Reference

Ackerman, S.A., 1989. Using the radiative temperature difference at 3.7 and 11 μm to tract dust outbreaks. Remote Sens Environ. 27, pp. 129-33. https://doi.org/10.1016/0034-4257(89)90012-6

Ackerman, S.A., 1997. Remote sensing aerosols using satellite infrared observations. Journal of Geophysical Research: Atmospheres. 102, pp. 17069-79. https://doi.org/10.1029/96JD03066

Ackerman, S.A., Chung, H., 1992. Radiative effects of airborne dust on regional energy budgets at the top of the atmosphere. Journal of Applied Meteorology. 31, pp. 223-33. https://doi.org/10.1175/1520-0450(1992)031<0223:REOADO>2.0.CO;2

Albugami, S., Palmer, S., Meersmans, J., Waine, T., 2018. Evaluating MODIS Dust-Detection Indices over the Arabian Peninsula. Remote Sensing. 10.

Ashpole, I., Washington, R., 2012. An automated dust detection using SEVIRI: A multiyear climatology of summertime dustiness in the central and western Sahara. Journal of Geophysical Research: Atmospheres. 117. https://doi.org/10.1029/2011jd016845

Baddock, M.C., Bullard, J.E., Bryant, R.G., 2009. Dust source identification using MODIS: a comparison of techniques applied to the Lake Eyre Basin, Australia. Remote Sens Environ. 113, pp. 1511-28. https://doi.org/10.1016/j.rse.2009.03.002

Bin Abdulwahed, A., Dash, J., Roberts, G., 2018. An evaluation of satellite dust-detection algorithms in the Middle East region. International Journal of Remote Sensing. pp. 1-26.

Bin Abdulwahed, A., Dash, J., Roberts, G., 2019. An evaluation of satellite dust-detection algorithms in the Middle East region. International Journal of Remote Sensing. 40, pp. 1331-56. https://doi.org/10.1080/01431161.2018.1524589

Butt, M.J., Mashat, A.S., 2018a. MODIS satellite data evaluation for sand and dust storm monitoring in Saudi Arabia. International Journal of Remote Sensing. 39, pp. 8627-45. https://doi.org/10.1080/01431161.2018.1488293

Butt, M.J., Mashat, A.S., 2018b. MODIS satellite data evaluation for sand and dust storm monitoring in Saudi Arabia. International Journal of Remote Sensing. 39, pp. 1-19. https://doi.org/10.1080/01431161.2018.1488293

Cecchi, G., Tramutoli, V., Zilioli, E., 1998. Robust AVHRR techniques (RAT) for environmental monitoring: theory and applications. Earth Surface Remote Sensing II pp. 101-13.

Chiapello, I., Prospero, J., Herman, J., Hsu, N., 1999. Detection of mineral dust over the North Atlantic Ocean and Africa with the Nimbus 7 TOMS. Journal of Geophysical Research: Atmospheres. 104, pp. 9277-91. https://doi.org/10.1029/1998JD200083

Coakley, J.A., Bretherton, F.P., 1982. Cloud cover from high‐resolution scanner data: Detecting and allowing for partially filled fields of view. Journal of Geophysical Research: Oceans. 87, pp. 4917-32. https://doi.org/10.1029/jc087ic07p04917

Coheur, P.-F., Barret, B., Turquety, S., Hurtmans, D., Hadji-Lazaro, J., Clerbaux, C., 2005. Retrieval and characterization of ozone vertical profiles from a thermal infrared nadir sounder. Journal of Geophysical Research: Atmospheres. 110. https://doi.org/10.1029/2005JD005845

Darmenov, A., Sokolik, I.N., 2005. Identifying the regional thermal‐IR radiative signature of mineral dust with MODIS. Geophysical Research Letters. 32. https://doi.org/10.1029/2005gl023092

El-Askary, H., Gautam, R., Singh, R.P., Kafatos, M., 2006. Dust storms detection over the Indo-Gangetic basin using multi sensor data. Advances in Space Research. 37, pp. 728-33. https://doi.org/10.1016/j.asr.2005.03.134

El-Askary, H., Kafatos, M., Liu, X., El-Ghazawi, T., 2003. Introducing new approaches for dust storms detection using remote sensing technology. IEEE International Geoscience and Remote Sensing Symposium, IEEE, Toulouse, France pp. 2439-41.

Ellrod, G.P., Connell, B.H., Hillger, D.W., 2003. Improved detection of airborne volcanic ash using multispectral infrared satellite data. Journal of Geophysical Research: Atmospheres. 108. https://doi.org/10.1029/2002jd002802

Evan, A.T., Heidinger, A.K., Pavolonis, M.J., 2006. Development of a new over‐water Advanced Very High Resolution Radiometer dust detection algorithm. International Journal of Remote Sensing. 27, pp. 3903-24. https://doi.org/10.1080/01431160600646359

Filonchyk, M., Yan, H., Yang, S., Lu, X., 2018. Detection of aerosol pollution sources during sandstorms in Northwestern China using remote sensed and model simulated data. Advances in Space Research. 61, pp. 1035-46. https://doi.org/10.1016/j.asr.2017.11.037

Ge, J., Huang, J., Weng, F., Sun, W., 2008. Effects of dust storms on microwave radiation based on satellite observation and model simulation over the Taklamakan desert. Atmospheric Chemistry and Physics. 8, pp. 4903-9. https://doi.org/10.5194/acp-8-4903-2008

Goudie, A.S., Middleton, N.J., 2006. Desert dust in the global system. Springer Science & Business Media, Berlin, Heidelberg 1-11 pp.

Hao, X., Qu, J.J., 2007. Saharan dust storm detection using moderate resolution imaging spectroradiometer thermal infrared bands. Journal of Applied Remote Sensing. 1, p. 013510. https://doi.org/10.1117/1.2740039

Herman, J., Celarier, E., 1997. Earth surface reflectivity climatology at 340–380 nm from TOMS data. Journal of Geophysical Research: Atmospheres. 102, pp. 28003-11. https://doi.org/10.1029/97jd02074

Hong, S., 2009. Detection of Asian dust (Hwangsa) over the Yellow Sea by decomposition of unpolarized infrared reflectivity. Atmospheric Environment. 43, pp. 5887-93. https://doi.org/10.1016/j.atmosenv.2009.08.024

Hu, X.Q., Lu, N.M., Niu, T., Zhang, P., 2008. Operational retrieval of Asian sand and dust storm from FY-2C geostationary meteorological satellite and its application to real time forecast in Asia. Atmos. Chem. Phys. 8, pp. 1649-59. https://doi.org/10.5194/acpd-7-8395-2007

Huang, J., Ge, J., Weng, F., 2007. Detection of Asia dust storms using multisensor satellite measurements. Remote Sens Environ. 110, pp. 186-91. https://doi.org/10.1016/j.rse.2007.02.022

Jankowiak, I., Tanré, D., 1992. Satellite Climatology of Saharan Dust Outbreaks: Method and Preliminary Results. Journal of Climate. 5, pp. 646-56. https://doi.org/10.1175/1520-0442(1992)005<0646:scosdo>2.0.co;2

Karimi, N., Moridnejad, A., Golian, S., Vali Samani, J.M., Karimi, D., Javadi, S., 2012. Comparison of dust source identification techniques over land in the Middle East region using MODIS data. Canadian Journal of Remote Sensing. 38, pp. 586-99. https://doi.org/10.5589/m12-048

Kazi A, K., Nagatani, I., Kawano, K., Kudoh, J.-I., 2018. Development of a new dust index NDLI for Asian dust extraction system based on Aqua MODIS data and monitoring of trans-boundary Asian dust events in Japan. International Journal of Remote Sensing. pp. 1-18. https://doi.org/10.1080/01431161.2018.1524170

Kazi A, K., Nagatani, I., Kawano, K., Kudoh, J.-I., 2019. Development of a new dust index NDLI for Asian dust extraction system based on Aqua MODIS data and monitoring of trans-boundary Asian dust events in Japan. International Journal of Remote Sensing. 40, pp. 1030-47. https://doi.org/10.1080/01431161.2018.1524170

Kim, H., Zohaib, M., Cho, E., Kerr, Y.H., Choi, M., 2017. Development and Assessment of the Sand Dust Prediction Model by Utilizing Microwave-Based Satellite Soil Moisture and Reanalysis Datasets in East Asian Desert Areas. Advances in Meteorology. 2017. https://doi.org/10.1155/2017/1917372

Landgraf, J., Hasekamp, O.P., 2007. Retrieval of tropospheric ozone: The synergistic use of thermal infrared emission and ultraviolet reflectivity measurements from space. Journal of Geophysical Research: Atmospheres. 112. https://doi.org/10.1029/2006JD008097

Legrand, M., Plana‐Fattori, A., N'doumé, C., 2001. Satellite detection of dust using the IR imagery of Meteosat: 1. Infrared difference dust index. Journal of Geophysical Research: Atmospheres. 106, pp. 18251-74. https://doi.org/10.1029/2000JD900749

Liu, Y., Liu, R., Cheng, X., 2013. Dust detection over desert surfaces with thermal infrared bands using dynamic reference brightness temperature differences. Journal of Geophysical Research: Atmospheres. 118, pp. 8566-84. https://doi.org/10.1002/jgrd.50647

Man-Hae, K., Omar, A.H., Tackett, J.L., Vaughan, M.A., Winker, D.M., Trepte, C.R., Hu, Y., Liu, Z., Poole, L.R., Pitts, M.C.J.A.M.T., 2018. The CALIPSO version 4 automated aerosol classification and lidar ratio selection algorithm. 11, p. 6107.

Marchese, F., Sannazzaro, F., Falconieri, A., Filizzola, C., Pergola, N., Tramutoli, V., 2017. An enhanced satellite-based algorithm for detecting and tracking dust outbreaks by means of SEVIRI data. Remote Sensing. 9, p. 537.

Martins, J.V., Tanré, D., Remer, L., Kaufman, Y., Mattoo, S., Levy, R., 2002. MODIS Cloud screening for remote sensing of aerosols over oceans using spatial variability. Geophysical Research Letters. 29, pp. MOD4-1-MOD4-. https://doi.org/10.1029/2001gl013252

Meskhidze, N., Chameides, W., Nenes, A., 2005. Dust and pollution: a recipe for enhanced ocean fertilization? Journal of Geophysical Research: Atmospheres. 110. https://doi.org/10.1029/2004JD005082

Miller, S.D., Bankert, R.L., Solbrig, J.E., Forsythe, J.M., Noh, Y.J., Grasso, L.D., 2017. A Dynamic Enhancement With Background Reduction Algorithm: Overview and Application to Satellite‐Based Dust Storm Detection. Journal of Geophysical Research: Atmospheres. 122.

Muhammad, A., Sheltami, T.R., Mouftah, H.T., 2012. A review of techniques and technologies for sand and dust storm detection. Reviews in Environmental Science and Bio/Technology. 11, pp. 305-22.

Norton, C.C., Mosher, F.R., Hinton, B., Martin, D.W., Santek, D., Kuhlow, W., 1980. A Model for Calculating Desert Aerosol Turbidity over the Oceans from Geostationary Satellite Data. Journal of Applied Meteorology. 19, pp. 633-44. https://doi.org/10.1175/1520-0450(1980)019<0633:Amfcda>2.0.Co;2

Park, S.S., Kim, J., Lee, J., Lee, S., Kim, J.S., Chang, L.S., Ou, S., 2014. Combined dust detection algorithm by using MODIS infrared channels over East Asia. Remote Sens Environ. 141, pp. 24-39. https://doi.org/10.1016/j.rse.2013.09.019

Potts, R., 1993. Satellite observations of Mt Pinatubo ash clouds. Australian Meteorological Magazine. 42.

Prachi, M.S., Pravin, K.D., 2014. Detection and monitoring of two dust storm events by multispectral MODIS images. Journal of Environmental Research and Development. 8, p. 974. https://doi.org/10.3724/sp.j.1146.2007.00469

Prata, A., 1989. Observations of volcanic ash clouds in the 10-12 μm window using AVHRR/2 data. International journal of Remote sensing. 10, pp. 751-61. https://doi.org/10.1080/01431168908903916

Prata, F., Bluth, G., Rose, B., Schneider, D., Tupper, A., 2001. Comments on “Failures in detecting volcanic ash from a satellite-based technique”. Remote Sens Environ. 78, pp. 341-6. https://doi.org/10.1016/s0034-4257(99)00103-0

Qu, J.J., Hao, X., Kafatos, M., Wang, L., 2006. Asian dust storm monitoring combining Terra and Aqua MODIS SRB measurements. IEEE Geoscience and Remote Sensing Letters. 3, pp. 484-6. https://doi.org/10.1109/lgrs.2006.877752

Rivas-Perea, P., PRosiles, J., Chacon, M., 2010a. Traditional and neural probabilistic multispectral image processing for the dust aerosol detection problem. Image Analysis & Interpretation (SSIAI), 2010 IEEE Southwest Symposium on Image Analysis & Interpretation (SSIAI), IEEE pp. 169-72.

Rivas-Perea, P., Rosiles, J., Cota-Ruiz, J., 2013. Statistical and neural pattern recognition methods for dust aerosol detection. International journal of remote sensing. 34, pp. 7648-70.

Rivas-Perea, P., Rosiles, J.G., Murguia, M.I.C., Tilton, J.J., 2010b. Automatic dust storm detection based on supervised classification of multispectral data. Soft Computing for Recognition Based on Biometrics, Springer pp. 443-54.

Roskovensky, J., Liou, K., 2003. Detection of thin cirrus from 1.38 μm/0.65 μm reflectance ratio combined with 8.6–11 μm brightness temperature difference. Geophysical Research Letters. 30. https://doi.org/10.1029/2003gl018135

Roskovensky, J., Liou, K., 2005. Differentiating airborne dust from cirrus clouds using MODIS data. Geophysical Research Letters. 32. https://doi.org/10.1029/2005gl022798

Samadi, M., Boloorani, A.D., Alavipanah, S.K., Mohamadi, H., Najafi, M.S., 2014. Global dust Detection Index (GDDI); a new remotely sensed methodology for dust storms detection. Journal of Environmental Health Science and Engineering. 12, p. 20. https://doi.org/10.1186/2052-336X-12-20

Sannazzaro, F., Filizzola, C., Marchese, F., Corrado, R., Paciello, R., Mazzeo, G., Pergola, N., Tramutoli, V., 2014. Identification of dust outbreaks on infrared MSG-SEVIRI data by using a Robust Satellite Technique (RST). Acta Astronautica. 93, pp. 64-70. https://doi.org/10.1016/j.actaastro.2013.07.003

Schuster, G.L., Dubovik, O., Holben, B.N.J.J.o.G.R.A., 2006. Angstrom exponent and bimodal aerosol size distributions. 111.

Shahrisvand, M., Akhoondzadeh, M., 2013. A Comparison of Empirical and Inteligent Methods for Dust Detection Using Modis Satellite Data. Remote Sensing and Spatial Information Sciences. 40-1-W3, pp. 371-5. https://doi.org/10.5194/isprsarchives-xl-1-w3-371-2013

Shao, Y., Dong, C.H., 2006. A review on East Asian dust storm climate, modelling and monitoring. Global and Planetary Change. 52, pp. 1-22. https://doi.org/10.1016/j.gloplacha.2006.02.011

She, L., Xue, Y., Yang, X., Guang, J., Li, Y., Che, Y., Fan, C., Xie, Y., 2018. Dust Detection and Intensity Estimation Using Himawari-8/AHI Observation. Remote Sensing. 10, p. 490. https://doi.org/10.3390/rs10040490

Shi, L., Zhang, J., Zhang, D., Igbawua, T., Liu, Y., 2019. Developing a dust storm detection method combining Support Vector Machine and satellite data in typical dust regions of Asia. Advances in Space Research. http://www.sciencedirect.com/science/article/pii/S027311771930835X

Shi, P., Song, Q., Patwardhan, J., Zhang, Z., Wang, D.J., 2018. Mineral Dust Detection Using Satellite Data.

Slanina, J., 2007. Air pollution: the emission–effect relation. Reviews in Environmental Science and Bio/Technology. 6, pp. 353-74. https://doi.org/10.1007/s11157-006-0017-9

Souri, A.H., Vajedian, S., 2015. Dust storm detection using random forests and physical-based approaches over the Middle East. Journal of Earth System Science. 124, pp. 1127-41.

Su, Q., Sun, L., Yang, Y., Zhou, X., Li, R., Jia, S., 2017. Dynamic Monitoring of the Strong Sandstorm Migration in Northern and Northwestern China via Satellite Data. Aerosol and Air Quality Research. 17, pp. 3244-52. https://doi.org/10.4209/aaqr.2016.12.0600

Taghavi, F., Owlad, E., Ackerman, S., 2017. Enhancement and identification of dust events in the south-west region of Iran using satellite observations. Journal of Earth System Science. 126, p. 28.

Torres, O., Bhartia, P., Herman, J., Ahmad, Z., Gleason, J., 1998. Derivation of aerosol properties from satellite measurements of backscattered ultraviolet radiation: Theoretical basis. Journal of Geophysical Research: Atmospheres. 103, pp. 17099-110. https://doi.org/10.1029/98JD00900

Torres, O., Tanskanen, A., Veihelmann, B., Ahn, C., Braak, R., Bhartia, P.K., Veefkind, P., Levelt, P., 2007. Aerosols and surface UV products from Ozone Monitoring Instrument observations: An overview. Journal of Geophysical Research: Atmospheres. 112. https://doi.org/10.1029/2007JD008809

Tramutoli, V., 2007. Robust satellite techniques (RST) for natural and environmental hazards monitoring and mitigation: Theory and applications. 2007 International Workshop on the Analysis of Multi-temporal Remote Sensing Images, IEEE, Leuven, Belgium pp. 1-6.

Tramutoli, V., Filizzola, C., Marchese, F., Mazzeo, G., Paciello, R., Pergola, N., Pietrapertosa, C., Sannazzaro, F., 2010. A Robust Satellite Technique (RST) for dust storm detection and monitoring: The case of 2009 Australian event. Geoscience and Remote Sensing Symposium (IGARSS), 2010 IEEE International, IEEE, Honolulu, HI, USA pp. 1707-9.

Varga, G., Újvári, G., Kovács, J., 2014. Spatiotemporal patterns of Saharan dust outbreaks in the Mediterranean Basin. Aeolian Research. 15, pp. 151-60. https://doi.org/10.1016/j.aeolia.2014.06.005

Verge-Depre, G., Legrand, M., Moulin, C., Alias, A., Francois, P., 2006. Improvement of the detection of desert dust over the Sahel using METEOSAT IR imagery. Annals Geophysicae pp. 2065-73.

Wald, A.E., Kaufman, Y.J., Tanré, D., Gao, B.C., 1998. Daytime and nighttime detection of mineral dust over desert using infrared spectral contrast. Journal of Geophysical Research: Atmospheres. 103, pp. 32307-13. https://doi.org/10.1029/98JD01454

Weger, M., Heinold, B., Engler, C., Schumann, U., Seifert, A., Fößig, R., Voigt, C., Baars, H., Blahak, U., Borrmann, S., 2018. The impact of mineral dust on cloud formation during the Saharan dust event in April 2014 over Europe. Atmospheric Chemistry and Physics. 18, pp. 17545-72. https://doi.org/10.5194/acp-18-17545-2018

William, E.S., Robert, J.C., 1974. The Detection of Dust Storms Over Land and Water With Satellite Visible and Infrared Measurements. Monthly Weather Review. 102, pp. 830-7. https://doi.org/10.1175/1520-0493(1974)102<0830:TDODSO>2.0.CO;2

Wong, M.S., Nichol, J.E., Lee, K.H., 2011. An operational MODIS aerosol retrieval algorithm at high spatial resolution, and its application over a complex urban region. Atmospheric Research. 99, pp. 579-89.

Xie, Y., Zhang, W., Qu, J., 2017. Detection of asian dust storm using MODIS measurements. Remote Sensing. 9, p. 869.

Xu, D., Qu, J.J., Niu, S., Hao, X., 2011a. Sand and dust storm detection over desert regions in China with MODIS measurements. International Journal of Remote Sensing. 32, pp. 9365-73. https://doi.org/10.1080/01431161.2011.556679

Xu, D., Qu, J.J., Niu, S., Hao, X., 2011b. Sand and dust storm detection over desert regions in China with MODIS measurements**. International Journal of Remote Sensing. 32, pp. 9365-73. https://doi.org/10.1080/01431161.2011.556679

Yan, X., Luo, N., Liang, C., Zang, Z., Zhao, W., Shi, W., 2020. Simplified and Fast Atmospheric Radiative Transfer model for satellite-based aerosol optical depth retrieval. Atmospheric Environment. 224, p. 117362. http://www.sciencedirect.com/science/article/pii/S1352231020301011

Yue, H., He, C., Zhao, Y., Ma, Q., Zhang, Q., 2017. The brightness temperature adjusted dust index: An improved approach to detect dust storms using MODIS imagery. International Journal of Applied Earth Observation and Geoinformation. 57, pp. 166-76. https://doi.org/10.1016/j.jag.2016.12.016

Zhao, T.X.P., Ackerman, S., Guo, W., 2010. Dust and Smoke Detection for Multi-Channel Imagers. Remote Sensing. 2, pp. 2347-68. https://doi.org/10.3390/rs2102347

Conflicts of interest:

The authors declare no conflicts of interest.